Available online at www.sciencedirect.com
SCIENCE DIRECT®
International Journal of Heat and Mass Transfer 47 (2004) 4101–4112
International Journal of HEAT and MASS TRANSFER
www.elsevier.com/locate/ijhmt

Rayleigh Bénard convective instability of a fluid under high-frequency vibration

I. Cisse, G. Bardan *, A. Mojtabi

UPS-IMFT, UFR MIG, Département de Mécanique, 118 route de Narbonne, 31000 Toulouse, France

Received 2 September 2003; received in revised form 10 May 2004
Available online 2 July 2004

Abstract

The generation of two-dimensional thermal convection induced simultaneously by gravity and high-frequency vibration in a bounded rectangular enclosure or in a layer is investigated theoretically and numerically. The horizontal walls of the container are maintained at constant temperatures while the vertical boundaries are thermally insulated, impermeable and adiabatic. General equations for the description of the time-averaged convective flow and, within this framework, the generalized Boussinesq approximation are formulated. These equations are solved using a spectral collocation method to study the influence of vibrations (angle and intensity). Hence, a theoretical study shows that mechanical quasi-equilibrium (i.e., state in which the averaged velocity is zero but the oscillatory component is in general non-zero) is impossible when the direction of vibration is not parallel to the temperature gradient. In the other case, it is proved that the mechanical equilibrium is linearly stable up to a critical value of the unique stability parameter, which depends on the vibrational field. In this paper, it is shown that high-frequency vertical oscillations can delay convective instabilities and, in this way, reduce the convective flow. The isotherms are oriented perpendicular to the axis of vibration. In the case where the direction of vibration is perpendicular to the temperature gradient, small values of the Grashof number, the stability parameter, induce the generation of an average convective flow. When the aspect ratio is large enough, the character of the bifurcation is practically the same as in the limiting case of an infinitely long layer.

Keywords: Vibration; Rayleigh Bénard

1. Introduction

Vibrations are known to be among the most effective ways of affecting the behaviour of fluid systems, in the sense of increasing or reducing the convective heat transfer. Most of the material in this paper is devoted to the case of high-frequency vibration (i.e., when the period of vibration is much smaller than the reference hydrodynamic times and the displacement amplitude is smaller than the height of the cell). We focus our attention on the case where a container filled with a fluid heated from below is subjected to arbitrary high-frequency vibrations. The description of the thermo-vibrational flows in the limiting case of high-frequency and small amplitude of vibrations may be effectively obtained in the frame of the averaging method, which leads to the system of equations for averaged fields of velocity, pressure and temperature. Simonenko et al. [1,2], were the first to use this method and propose the time-averaged form of the Boussinesq equations. Subsequently, it was demonstrated that high-frequency vibrations are most relevant in modifying stability characteristics. Gershuni and Zhukhovitskii [3] introduced the vibrational analogue of the Rayleigh Number, Ra_v, to represent the intensity of the vibrational source.

* Corresponding author. Tel.: +33-5-61-55-6788; fax: +33-5-61-55-8326.
E-mail address: bardan@imft.fr (G. Bardan).

0017-9310/$ - see front matter © 2004 Elsevier Ltd. All rights reserved.
doi:10.1016/j.ijheatmasstransfer.2004.05.002

Thus, for an infinite fluid layer in weightlessness (i.e., when the static gravity is absent), only the specific thermovibrational mechanism is responsible for instability excitation and quasi-equilibrium is possible. They studied the effects of vibration angle and the interaction between natural and thermovibrational convection. The configuration corresponding to a horizontal layer heated from below or from above under longitudinal vibration is considered by Braverman and Oron [4] and by Gershuni and Zhukhovitskii [3]. They show that the state of quasi-equilibrium becomes unstable when the vibrational Rayleigh number exceeds some critical value which depends on the boundary conditions at the parallel planes bounding the fluid layer. At a given α (angle between axis of vibration and isothermal surfaces), the neutral curve $Ra_v(k)$ assumes a minimum at some k_c which determines the wave number of the most dangerous perturbation. The corresponding value Ra_{v_c} yields the equilibrium stability border. The numerical calculation implies that the stability is minimal for longitudinal vibrations for $Ra_{v_c} = 2129$ and $k_c = 3.23$. The critical value of the vibrational Rayleigh number increases monotonically with the angle of inclination of the vibration axis. When $\alpha \to \frac{\pi}{2}$, they found $Ra_{v_c} \to \infty$ and $k_c \to 0$. In the presence of static gravity, the onset of convection is caused by both thermovibrational and thermogravitational mechanisms. Several examples involving both mechanisms were presented by Gershuni and Zhukhovitskii [5] and later by Braverman and Oron [4]. The experimental results given by Zavarykin et al. [6] are in good agreement with the theoretical ones. Thermovibrational convection in an enclosure has long been investigated during the last decade due to its extensive applications in engineering, like solar energy systems, electronic cooling equipment or crystal growth processes. There are many practical problems of natural convection in an enclosure which are caused by non-periodic (accelerating–decelerating) or periodic (harmonic vibration) motion. In the past, Richardson [7] reviewed the effects of sound and wall vibration on heat transfer. Forbes et al. [8] conducted experiments to investigate the enhancement of thermal convection heat transfer in a liquid-filled rectangular enclosure by vibration. The results showed that the vibration frequency and acceleration were the dominant factors that affected heat transfer.

Using the time averaged method, Gershuni and Zhukhovitskii [5] studied the vibrational thermal convection under weightlessness in a rectangular, cylindrical enclosure and a heated cylinder in an unconfined fluid. Due to the high frequency assumption, many important phenomena, like the resonant state and the detailed variation of the heat transfer rate could not be investigated. However, Yurkov [9] directly solved the Boussinesq-approximated governing equations to study the thermal convection induced by finite-frequency vibration under weightless conditions. From the results of the average Nusselt number, the parametric resonant phenomenon was found. A more exhaustive study was carried out by Fu and Shieh [10] to investigate the effects of the vibration frequency and Rayleigh number on the thermal convection in the enclosure. The vibration frequency was varied from 1 to 10^4 and three different values of the Rayleigh number were considered. According to the results, thermal convection can be divided into five regions: (i) quasi-static convection, (ii) vibration convection, (iii) resonant vibration convection, (iv) intermediate convection and (v) high-frequency vibration convection. When the Rayleigh number is large enough, ($Ra = 10^6$), gravitational thermal convection dominates, and the vibration motion does not markedly enhance the heat transfer rate. In contrast, in the low Rayleigh number ($Ra = 10^4$) case, except in the quasi-static convection region, the vibration thermal convection is dominant, and the vibration enhances the heat transfer significantly. So, Gershuni et al. [11], in studying the structures of the flows, report that the transition from the basic to a multicellular flow sets in at a critical value of the Ra_v. When the aspect ratio equals 8 or more, the character of the bifurcation is practically the same as in the limiting case of an infinitely long layer. The latter statement was confirmed by Khallouf et al. [12], Lizée [13], Bardan et al. [14] for a binary mixture when they studied the non-linear regimes of two-dimensional thermovibrational convection in rectangular cavities subjected to a longitudinal temperature gradient and transversal axis of vibration. It was shown that the transition from a four-vortex regime to inversional symmetry took place at some critical value of Ra_v. This value increased monotonously as the aspect ratio A_L increased. Thus, when $A_L \gg 4$, the limiting case of rest with conductive heat transfer occurred.

All these previous results were of great help for understanding the g-jitter effects during fluid and material science microgravity experiments. On available space platforms, a systematic characterization of the accelerations has shown that the microgravity environment is dynamic, depending on many sources, e.g., aerodynamic forces, on-board machinery, crew operations or servicing activities. It is recognized that the presence of g-disturbances may cause strong discrepancies, and so, the fluid science processes may be substantially changed by g-disturbances. To reduce the convective contributions of these g-jitters, it is convenient to consider acceleration fields as an expansion of harmonic oscillations, and to use a time-averaged method formulation. Previously, there have been many studies on thermal convection in a gravitationally modulated fluid layer with rigid, isothermal boundaries heated from below or from above, see Gresho and Sani [15], Rosenblat and Tanaka [16]. Biringen and Danabasoglu [17] studied the effects of gravity modulation in

a thermally driven rectangular enclosure for terrestrial and microgravity environments. The results showed that the destabilizing and stabilizing effects of gravity modulation agreed with the theories of Gresho and Sani [15]. More recently, Monti and Savino [18,19] performed a numerical simulation of non-linear problems of TVC (thermovibrational convection) with reference to typical fluid science experiments on the space station. They established that the flow field is in general 3D, because of end wall effects and the heat exchange with the surroundings through the lateral walls (not perfectly insulated). In the case of g-jitter, we have to deal with multifrequency vibrations spanning the interval from 10^{-1} to 10^{3}, and here too, a time averaged formulation is necessary in order to reduce the computation time. Savino et al. [20] have also studied a three-dimensional TVC in a closed cell filled with liquid, with an initial linear temperature and a g-jitter orthogonal to the density gradient. They revealed that the time-averaged convective motion due to thermovibrational effects arises because of non-linear coupling between density and acceleration oscillations. The 3D numerical results presented in their work in terms of velocity and temperature fields are helpful for the design of microgravity experiments and to evaluate the range of validity of the two-dimensional assumption invoked in previous calculations.

Our study concerns the effects of vibration in a finite rectangular box filled with fluid. Our aim is to understand the effects of g-jitter on this problem. We also deal with an unbounded layer filled with fluid subjected to a horizontal or vertical vibrational field. We restrict our work to the case of a pure fluid but we add the influence of arbitrary angles of vibration. In studying the equilibrium conditions, we have found general equations for the quasi-equilibrium and equilibrium states. According to the boundary conditions applied to different geometries, it is possible to know if quasi-equilibrium or equilibrium exists. Many of our stability results are concerned with a vibrational parameter which depends only on the vibrational effects (i.e., it does not depend on temperature difference). In comparison with previous works which deal with the vibrational Grashof number, the use of this specific parameter permits a better understanding of the vibrational effects on convective flows. Numerical computations have been performed, too, in order to foresee the theoretical results.

2. Problem description and basic equations

We consider two-dimensional thermovibrational convection in a container of height H and length L. Fig. 1 represents the flow configuration and coordinates system. The flow domain is $(x,z) \in \Omega = [0,L] \times [0,H]$. All the physical properties are taken to be constant. The

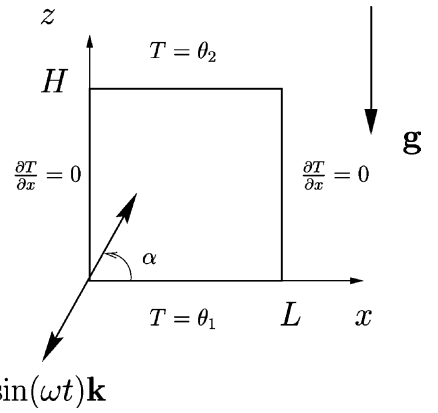

Fig. 1. Geometrical configuration and axis of coordinates. Sketch of the cavity configuration.

horizontal walls at $z = 0$ and $z = H$ are kept at constant and uniform temperatures θ_1 and θ_2, respectively. The situation where $\theta_1 > \theta_2$ is adopted. The vertical walls (at $x = 0$ and $x = L$) are insulated. All the boundaries are assumed rigid. The fluid cavity with its boundaries is subjected to linear harmonic oscillations.

2.1. The mathematical model

The fluid in the cavity is considered to be Newtonian and to satisfy the Boussinesq approximation. The thermophysical properties are constant except for the density in the buoyancy term which depends linearly on the local temperature. The equation of state has the form (1).

$$\rho(\theta) = \rho_{\mathrm{ref}}(1 - \beta_\theta(\theta - \theta_{\mathrm{ref}})) \tag{1}$$

where $\rho_{\mathrm{ref}} = \rho(\theta_{\mathrm{ref}})$ is the density at standard temperature $\theta_{\mathrm{ref}} = \theta_2$ and $\beta_\theta = \frac{-1}{\rho_{\mathrm{ref}}}\frac{\partial \rho}{\partial \theta}$ the thermal expansion coefficient. By introducing the appropriate coordinates connected with oscillating systems, the gravitational field is replaced by the sum of the gravitational and the vibrational acceleration (2) in the momentum equation.

$$\mathbf{g} \to \mathbf{g} - b\omega^2 \sin(\omega t)\,\mathbf{k} \tag{2}$$

where $\mathbf{k} = \cos\alpha\mathbf{x} + \sin\alpha\mathbf{z}$ is the unit vector along the axis of vibration and $\alpha = (\mathbf{x}, \mathbf{k})$ is the angle of vibration, b is the displacement amplitude and ω the angular frequency.

These hypotheses lead to the following dimensionless conservation equations for mass (3), momentum (4) and energy (5), with the Boussinesq approximation. Using the velocity $\mathbf{u}$, the pressure p and the temperature θ as independent variables, the non-dimensional equations of the Boussinesq model are

$$\nabla \cdot \mathbf{u} = 0 \tag{3}$$

$$\frac{\partial \mathbf{u}}{\partial t} + (\mathbf{u}\cdot\nabla)\mathbf{u} = -\nabla p + \nabla^2\mathbf{u} + Gr\,\theta\,\mathbf{z} + Gr_{\mathrm{v}}\,\theta\,\hat{\omega}\,\sin(\hat{\omega}t)\,\mathbf{k} \tag{4}$$

$$\frac{\partial \theta}{\partial t} + (\mathbf{u}\cdot\nabla)\theta = \frac{1}{Pr}\nabla^2\theta \tag{5}$$

In the above equations, using the viscous diffusion time as the time-scale factor, lengths are non-dimensionalized by H, velocity by $\frac{\nu}{H}$ (ν is the kinematic diffusivity), time by $\frac{H^2}{\nu}$, ω by $\frac{\nu}{H^2}$ and temperature relative to θ_2 by $\theta_1-\theta_2$. In line with the problem description, the corresponding non-dimensional forms of the boundary conditions are (6)–(9).

$$\mathbf{u} = \mathbf{0} \quad \text{on } \partial\Omega \tag{6}$$

$$\theta = 1 \quad \text{for } z = 0, \forall x \tag{7}$$

$$\theta = 0 \quad \text{for } z = 1, \forall x \tag{8}$$

$$\frac{\partial \theta}{\partial x} = 0 \quad \text{for } x = 0 \text{ and } A_{\mathrm{L}}, \forall z \tag{9}$$

The problem includes five non-dimensional numbers; the Grashof number $Gr = \frac{g\beta_\theta(\theta_1-\theta_2)H^3}{\nu^2}$, the modified vibrational Grashof number $Gr_{\mathrm{v}} = \frac{b\omega\beta_\theta(\theta_1-\theta_2)H}{\nu}$, the pulsation $\hat{\omega} = \omega\frac{H^2}{\nu}$, the Prandtl number $Pr = \frac{\nu}{a}$ (a is the heat diffusivity) and the aspect ratio $A_{\mathrm{L}} = \frac{L}{H}$. The modified vibrational Grashof number is obtained by substituting g by $b\omega^2$ in the Grashof number and rescaling by the ratio between the viscous diffusive time and the vibrational time $\frac{H^2/\nu}{1/\omega}$. In the limit of high-frequency and low amplitude, the effect of vibration is then determined by the product $b\omega$ which appears in the definition of the modified vibrational Grashof number Gr_{v}.

2.2. The averaged flow equations

In the asymptotic case of high-frequency oscillations where the period of the displacement $\tau = \frac{2\pi}{\omega}$ is very low compared to the characteristic times of thermal and kinematic diffusion ($\tau \ll \frac{H^2}{a}$ and $\tau \ll \frac{H^2}{\nu}$) the application of the averaging method of Simonenko [2] only allows the mean flow and mean temperature to be solved (see [21]).

Let us introduce the additional variable $\mathbf{W}$ which forms the solenoidal part of the temperature field contribution to the gravitational force and $\nabla\xi$ its conservative part in the following Helmholtz decompositions (10) and (11).

$$T\,\mathbf{k} = \mathbf{W} + \nabla\xi \tag{10}$$

$$\nabla\cdot\mathbf{W} = 0 \tag{11}$$

The mean motion is then determined by (12)–(16).

$$\nabla\cdot\mathbf{U} = 0 \tag{12}$$

$$\frac{\partial \mathbf{U}}{\partial t} + (\mathbf{U}\cdot\nabla)\mathbf{U} = -\nabla P + \nabla^2\mathbf{U} + GrT\,\mathbf{z} + \frac{1}{2}Gr_{\mathrm{v}}^2\mathbf{W}\cdot\nabla(T\mathbf{k}-\mathbf{W}) \tag{13}$$

$$\frac{\partial T}{\partial t} + (\mathbf{U}\cdot\nabla)T = \frac{1}{Pr}\nabla^2 T \tag{14}$$

$$\nabla T \wedge \mathbf{k} = \nabla \wedge \mathbf{W} \tag{15}$$

$$\nabla.\mathbf{W} = 0 \tag{16}$$

The boundary conditions are in accordance with the physical statement of the problem being (6)–(9) and (17):

$$\mathbf{W}\cdot\mathbf{n} = 0 \quad \text{on } \partial\Omega \tag{17}$$

where $\mathbf{n}$ is the outside normal vector.

3. Linear stability

3.1. Mechanical equilibrium

An equilibrium solution in presence of an oscillating force is possible only under certain conditions of heat input and cavity shape. In this case, the time averaged body force is compensated by the pressure gradient. The question is whether the state of mechanical quasi-equilibrium (i.e., the state at which the mean velocity is zero, but the pulsational component is not in general) exists or not in our situation. In order to prove the existence of a pure conductive solution of the systems (12)–(16), we substitute $\mathbf{U} = U_x\mathbf{x} + U_z\mathbf{z} = 0$ and $\frac{\partial}{\partial t} = 0$, the equilibrium fields $T = T_0$, $\mathbf{W} = \mathbf{W_0}$ and $P = P_0$ in this system and seek a valid solution for arbitrary values of the non-dimensional parameters. The following system (18)–(21) is obtained:

$$-\nabla P_0 + GrT_0\,\mathbf{z} + \frac{1}{2}Gr_{\mathrm{v}}^2\mathbf{W}_0\cdot\nabla(T_0\mathbf{k}-\mathbf{W}_0) = 0 \tag{18}$$

$$\Delta T_0 = 0 \tag{19}$$

$$\nabla T_0 \wedge\ \mathbf{k} = \nabla\wedge\mathbf{W}_0 \tag{20}$$

$$\nabla\cdot\mathbf{W}_0 = 0 \tag{21}$$

with the boundary conditions (22)–(25):

$$T_0 = 1 \quad \text{for } z = 0, \forall x \tag{22}$$

$$T_0 = 0 \quad \text{for } z = 1, \forall x \tag{23}$$

$$\frac{\partial T_0}{\partial x} = 0 \quad \text{for } x = 0 \text{ and } A_{\mathrm{L}}, \forall z \tag{24}$$

$$\mathbf{W}_0\cdot\mathbf{n} = 0 \quad \text{on } \partial\Omega. \tag{25}$$

Eq. (19) with boundary conditions (22) and (23) lead to $T_0 = 1 - z$. Applying the curl to Eq. (18), we obtain the vibrational hydrostatic condition (26):

$$\nabla(\mathbf{W}_0\cdot\mathbf{k})\wedge\nabla\ T_0 = 0 \tag{26}$$

The equilibrium follows from (19)–(21) and (26) when supplemented by the corresponding boundary conditions (specification of temperature and the requirement that $\mathbf{W}_0 \cdot \mathbf{n}$ vanishes on the cavity walls). Using the system of partial differential Eqs. (20)–(26), we can find the solenoidal vector $\mathbf{W}_0$ as indicated below:

$$\mathbf{W}_0 = \mathbf{W}_{0x}\mathbf{x} + \mathbf{W}_{0z}\mathbf{z} \qquad \text{where} \tag{27}$$

$$\mathbf{W}_{0x} = -\frac{1}{2}\sin(2\alpha)\,(x\cos\alpha + z\sin\alpha) - c_1 x\sin\alpha + c_1 z\cos\alpha + c \tag{28}$$

$$\mathbf{W}_{0z} = \cos^2(\alpha)\,(x\cos\alpha + z\sin\alpha) + c_1 x\cos\alpha + c_1 z\sin\alpha + c' \tag{29}$$

c_1, c, c' are integration constants. We specify that, in this general solution $\mathbf{W}_0$, the boundary conditions (25) are not taken into account.

3.1.1. Horizontal layer

Let us consider the problem of mechanical quasi-equilibrium stability for an infinite plane layer bounded by two parallel rigid plates $z = 0$ and 1. Taking boundary conditions (25) into account, the values of W_{0x} and W_{0z} (28), (29) lead to the following quasi-equilibrium solution

$$\mathbf{W}_0 \cdot \mathbf{z} = 0 \qquad \text{for } z = 0 \text{ and } z = 1. \tag{30}$$

$$T_0 = 1 - z \tag{31}$$

and

$$\frac{\partial \omega_{0x}}{\partial z} = -\cos\alpha \tag{32}$$

In this case, the solenoidal field is longitudinal. We suppose that the net flux of this field is equal zero, i.e. $\int_{z=0}^{z=1} \mathbf{W}_0 \cdot \mathbf{x}\mathrm{d}z = 0$ which leads to:

$$T_0 = 1 - z \tag{33}$$

$$\mathbf{W}_{0z} = 0 \tag{34}$$

$$\mathbf{W}_{0x} = \left(\frac{1}{2} - z\right)\cos\alpha \tag{35}$$

This solution for $\mathbf{W}_0$ has already been found by Gershuni and Lyubimov [21]. Therefore, we can conclude that quasi-equilibrium exists for an infinite plane layer subject to arbitrary angles of vibration.

3.1.2. Rectangular cavity

This situation is markedly different from that mentioned above. For arbitrary values of α ($\alpha \neq \frac{\pi}{2}$), the quasi-equilibrium solution or the equilibrium solution are not possible and the thermovibrational convective flow sets in at infinitely small values of temperature difference. In fact, if boundary conditions (25) are taken into account in Eqs. (28) and (29), we have an equilibrium solution only for $\alpha = \frac{\pi}{2}$. This equilibrium state under vertical vibration exists independently of the Grashof and vibrational Grashof number. Consequently, we will deal with arbitrary angles of vibration for an unbounded layer but only with vertical vibration for a container. In both cases, quasi-equilibrium or equilibrium solutions exist.

3.2. Stability of the equilibrium solution

In the following we write $G_v = \frac{1}{2}Gr_v^2$ and refer to it as the vibrational Grashof number.

It is convenient to rewrite mean field Eqs. (12)–(16) as evolution equations for two-dimensional perturbations about this equilibrium state. We denote these perturbations by $(\mathbf{U}', P', T', \mathbf{W}')$ and introduce the following streamfunction representations

$$U_x' = -\frac{\partial \psi'}{\partial z} \quad \text{and} \quad U_z' = \frac{\partial \psi'}{\partial x} \tag{36}$$

$$W_x' = -\frac{\partial \phi'}{\partial z} \quad \text{and} \quad W_z' = \frac{\partial \phi'}{\partial x} \tag{37}$$

As a result a positive streamfunction corresponds to a clockwise cell i.e. $\mathbf{U}' = \mathrm{curl}(\psi'\mathbf{y})$.

3.3. Horizontal layer with arbitrary angle of vibration

Considering the mean field Eqs. (12)–(16), replacing the expressions U_x', U_z', W_x', W_z' defined in (36) and (37), and taking the curl of Eq. (13), the resulting equations are

$$\frac{\partial}{\partial t}\begin{pmatrix} \Delta\psi' \\ T' \\ 0 \end{pmatrix} = \begin{pmatrix} \Delta^2 & Gr\dfrac{\partial}{\partial x} & -G_v\dfrac{\partial^2}{\partial x^2} \\ \dfrac{\partial}{\partial x} & \dfrac{\Delta}{Pr} & 0 \\ 0 & \dfrac{\partial}{\partial x} & -\Delta \end{pmatrix}\begin{pmatrix} \psi' \\ T' \\ \phi' \end{pmatrix} + \begin{pmatrix} N_1(\psi',\psi') \\ N_3(\psi',T') \\ 0 \end{pmatrix} + G_v\begin{pmatrix} N_1(\phi'\phi') - N_2(\phi' T') \\ 0 \\ 0 \end{pmatrix} + G_v\left(\frac{1}{2} - z\right)\cos\alpha\begin{pmatrix} \dfrac{\partial}{\partial x}\left(\Delta\phi' - \dfrac{\partial T'}{\partial x}\right) \\ 0 \\ 0 \end{pmatrix} \tag{38}$$

where for all pairs (f, g) of real functions

$$N_1(f,f) = \frac{\partial f}{\partial z}\left(\frac{\partial^3 f}{\partial x \partial z^2} + \frac{\partial^3 f}{\partial x^3}\right) - \frac{\partial f}{\partial x}\left(\frac{\partial^3 f}{\partial x^2 \partial z} + \frac{\partial^3 f}{\partial z^3}\right) \tag{39}$$

$$N_2(f,g)=\frac{\partial^2 f}{\partial x\partial z}\frac{\partial g}{\partial x}+\frac{\partial f}{\partial z}\frac{\partial^2 g}{\partial x^2}-\frac{\partial^2 f}{\partial x^2}\frac{\partial g}{\partial z}-\frac{\partial f}{\partial x}\frac{\partial^2 g}{\partial x\partial z} \quad (40)$$

$$N_3(f,g)=\frac{\partial f}{\partial z}\frac{\partial g}{\partial x}-\frac{\partial f}{\partial x}\frac{\partial g}{\partial z} \quad (41)$$

The associated boundary conditions are

$$\left(\frac{\partial \psi'}{\partial z}\right)_{z=0,1}=\left(\psi'\right)_{z=0,1}=0 \quad (42)$$

$$(T')_{z=0,1}=0 \quad (43)$$

$$(\phi')_{z=0,1}=0 \quad (44)$$

3.3.1. Analytical results

The resulting linear problem is solved by means of a Galerkin method using the following expansions

$$\psi'=\sum_{i=1}^{N} a_i(z-1)^2 z^{i+1}\mathrm{e}^{Ikx}\mathrm{e}^{I\Omega_h t} \quad (45)$$

$$T'=\sum_{i=1}^{N} b_i(z-1)z^{i}\mathrm{e}^{Ikx}\mathrm{e}^{I\Omega_h t} \quad (46)$$

$$\phi'=\sum_{i=1}^{N} c_i(z-1)z^{i}\mathrm{e}^{Ikx}\mathrm{e}^{I\Omega_h t} \quad (47)$$

where Ω_h and k are real numbers, $I=\sqrt{-1}$ and $i\in IN$.

For an unbounded layer, the truncation used ($N=4$) predicts that $Ra_c=PrGr_c=1708.549$ and $k_c=3.116$. This result is in good agreement with the result ($Ra_c=PrGr_c=1707.762$) found by Reid and Harris [22]. Fig. 2 presents the linear stability results for vibration at angle α. In Fig. 2(a) we recover the results of Gershuni and Lyubimov [21]. The critical point on the $Ra=PrGr$ axis is the solution of the classic Rayleigh–Bénard problem. This critical Rayleigh number $Ra_c=1708$ is connected with the most dangerous perturbation of the wavenumber $k_c=3.116$. This point on the PrG_v axis corresponds to the case of pure weightlessness. In the range of inclination angles, the stability curves intersect the PrG_v axis and go to negative Ra. For Gershuni and Lyubimov [21], this means that instability occurs when a system is heated from above. In order to understand what can happen on earth, we propose a new formulation which will be adapted with an experiment. In an experiment on earth we can start in the static case $G_v=0$, increase the parietal temperature gradient ΔT and reach the critical Rayleigh number at which convection occurs. Then, for a fixed value of PrG_v, we do the same and increase ΔT from 0 to its critical value corresponding to the onset of convection. For a sufficiently large fixed value of PrG_v , the convection seems to occur at the beginning of the experimentation i.e. for $Ra=0$. As $Ra=Pr\frac{g\beta_0(\theta_1-\theta_2)H^3}{\nu^2}$ this means on earth that $\Delta T=(\theta_1-\theta_2)=0$ and it follows by definition that $G_v=0$. This is in contradiction with the fact that we can always impose a value of PrG_v and then increase ΔT. The problem comes from the formulation as both Ra and PrG_v depend on ΔT. By setting $G_v=G_v^*.Gr^2$ with $G_v^*=\frac{1}{2}\frac{b^2\omega^2\nu^2}{g^2H^4}$, the new adimensional vibrational parameter G_v^* no longer depends on ΔT. Fig. 2(b) presents the same stability borders but in the plane $(PrGr, PrG_v^*)$. This formulation is then adapted to an experimentation on earth. Moreover, a particular

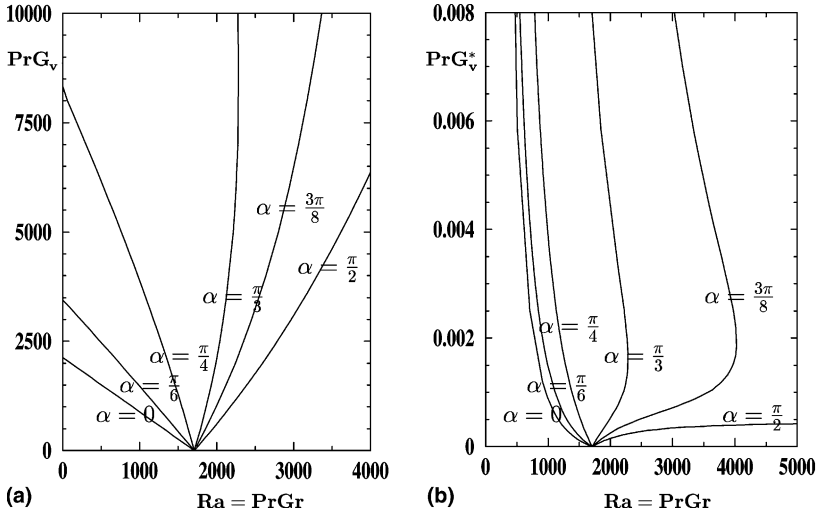

Fig. 2. (a) Stability borders in the plane (Ra, Pr^2G_v) for different inclination angles of the vibration axis (see [21]). (b) Stability borders in the plane (Ra, $Pr^2G_v^*$) for different inclination angles of the vibration axis. In the limiting case of high intensity of the vibrational field i.e. $b\omega^2\to\infty$ the system will have a behaviour closer and closer to the one it would have under zero-gravity conditions (except for $\alpha=\frac{\pi}{2}$).

angle of vibration is clearly shown. As one can see on Fig. 2(b), the stability borders for vertical vibrations ($\alpha = \frac{\pi}{2}$) are markedly different from the others. For $0 \leqslant \alpha \leqslant \alpha_c$ where $\alpha_c = \frac{27\pi}{100}$, Ra_c decreases with respect to G_v^* and $Ra_c \to 0$ when $G_v^* \to \infty$. For $\alpha_c \leqslant \alpha < \frac{\pi}{2}$, Ra_c first increases then decreases with respect to G_v^* but finally $Ra_c \to 0$ when $G_v^* \to \infty$. For $\alpha = \frac{\pi}{2}$, Ra_c increases with respect to G_v^* and $Ra_c \to \infty$ when $G_v^* \to \infty$. This different behaviour could be linked with the vertical sidewall effects in the presence of vibration. We have seen that mechanical quasi-equilibrium exists only for vertical vibration in a rectangular cavity, whereas it always exists for unbounded layers. This shows that, with vibration, an unbounded layer cannot exactly represent the physics of a very large rectangular cavity. In the following, we will keep the formulation in G_v as it is now classic (see the bibliography) in the studies of thermovibrational convection.

3.3.2. Stationary or oscillatory threshold

In the static case, the linear stability problem is determined by the product $PrGr$ which defines the Rayleigh number $Ra = PrGr$. Moreover, the linearized Eq. (38) are self-conjugated and the principle of stability exchange applies i.e. only steady state bifurcations occur.

With vibration, the linearized Eq. (38) are not self-conjugated and we cannot demonstrate that the bifurcations are always stationary. Nevertheless, for all the following results we have verified that no Hopf bifurcation occurs and Ω_h is found to be a pure imaginary complex in each case we have solved. We should mention that the associated Grashof number and also Ω_h strongly depend on the Prandtl number and the product $PrGr$ *is not relevant* for the oscillatory regime. To conclude, with vibration, only steady state bifurcations occur in the range of parameters (Pr, G_v) which we use in the following. In the framework of stationary bifurcations, the linear stability problem is, as in the static case, determined by $Ra = PrGr$ and $Ra_v = PrGr_v$. Within this formulation in Rayleigh number Ra, the Prandtl number Pr does not appear explicitly in the linear stability analysis except for Hopf bifurcation but we have seen there are none.

Nevertheless, we keep the formulation in terms of Grashof number Gr because it will be shown in the weakly non-linear analysis that the formulation in Rayleigh number is not sufficient to explicitly eliminate the Prandtl number.

3.4. Rectangular cavity and vertical vibration

For a cavity, the perturbation equations are also given by (38) but α must be set to $\alpha = \frac{\pi}{2}$.

At the boundaries of the cavity the streamfunctions vanish and thus

$$\left(\frac{\partial \psi'}{\partial x}\right)_{x=0,A_L} = \left(\frac{\partial \psi'}{\partial z}\right)_{z=0,1} = \left(\psi'\right)_{\partial\Omega} = 0 \tag{48}$$

$$T'_{z=0,1} = \left(\frac{\partial T'}{\partial x}\right)_{x=0,A_L} = 0 \tag{49}$$

$$(\phi')_{\partial\Omega} = 0 \tag{50}$$

In this case, we use the following expansions

$$\psi' = \sum_{i=1}^{N}\sum_{j=1}^{M} a_{ij}(x - A_L)^2 x^{i+1}(z-1)^2 z^{j+1} e^{I\Omega_h t} \tag{51}$$

$$T' = \sum_{j=1}^{M} b_{0j}(z-1)z^j e^{I\Omega_h t} + \sum_{i=1}^{N}\sum_{j=1}^{M} b_{ij} \times \left(\frac{x}{i+2} - \frac{A_L}{i+1}\right) x^{i+1}(z-1)z^j e^{I\Omega_h t} \tag{52}$$

$$\phi' = \sum_{i=1}^{N}\sum_{j=1}^{M} c_{ij}(x - A_L)x^i(z-1)z^j e^{I\Omega_h t} \tag{53}$$

where Ω_h is a real number, $I = \sqrt{-1}$ and $(i,j) \in IN^2$.

Equation (38) with boundary conditions (48)–(50) are invariant under two reflections. These operations are described by the operators S_x, S_z and $S_o = S_x S_z$ defined by

$$S_x \begin{pmatrix} \psi' \\ T' \\ \psi'_1 \end{pmatrix}(x,z) = \begin{pmatrix} -\psi' \\ T' \\ -\psi'_1 \end{pmatrix}(A_L - x, z) \tag{54}$$

$$S_z \begin{pmatrix} \psi' \\ T' \\ \psi'_1 \end{pmatrix}(x,z) = \begin{pmatrix} -\psi' \\ -T' \\ -\psi'_1 \end{pmatrix}(x, 1-z) \tag{55}$$

$$S_o \begin{pmatrix} \psi' \\ T' \\ \psi'_1 \end{pmatrix}(x,z) = \begin{pmatrix} \psi' \\ -T' \\ \psi'_1 \end{pmatrix}(A_L - x, 1-z) \tag{56}$$

The different reflections S_x, S_o, S_z verify the relations $S_x^2 = Id$, $S_z^2 = Id$ and $S_o^2 = Id$. The representation Γ of the group $Z_2 \times Z_2$ is $\Gamma \equiv \{Id, S_x, S_z, S_o\}$, where Id is the identity operator and this group plays an important role in the bifurcation analysis described below. In the presence of this group, the conduction state can lose stability and bifurcate to one specific solution which possesses either S_o-symmetric, S_x-symmetric, S_z-symmetric or has all the symmetry properties. The resulting bifurcations are pitchforks except for the last case. Without vibration, it is known that S_z-symmetric solutions are always unstable and result from at least a second primary bifurcation. The first two primary bifurcations are supercritical pitchforks with either S_o-symmetric or S_x-symmetric solutions [23]. The S_x-symmetric eigenmodes contain an even number of rolls in the x-direction, whereas the S_z-symmetric ones contain an even number of rolls in the z-direction. The

S_o-symmetric eigenmodes contain an odd number of cells in both directions. The eigenmodes which possess all the symmetry properties contain an even number of cells in both directions. For the first primary bifurcation, the eigenvector could be either S_x-symmetric or S_o-symmetric. Moreover, for second primary bifurcation, the eigenvector could be either S_z-symmetric or have all the symmetry properties (S_o, S_x and S_z) but this solution could not be observed as it remains unstable almost without vibration.

MAPLE and MATLAB were used to find the values of Ra_c, Ω_{hc}, a_{ij}, b_{ij} and c_{ij} at which a bifurcation occurs.

The choice of the truncation used ($N = 6$ and $M = 6$) for a square cavity is linked with the results of Mizushima [23] who studied the static case. When the rectangle is long, it is convenient to take more test functions in the (Ox) direction in order to get a better convergence of the solution. For example, for $A_L = 5$, we took $N = 11$ and $M = 6$ (see Tables 1 and 2). The numerical computations confirm this choice. As shown in Fig. 3, our results are in good agreement with those of Mizushima [23].

Before presenting the influence of a vibrational field, it is worthwhile to recall the following well-known results concerning the static case. As previously mentioned, the conductive solution can lose stability to four different states that have different symmetry properties. The neutral curves of modes which have the same symmetry do not intersect. This repulsion of the eigenvalues was discussed by the stability of paths of symmetry-breaking bifurcations by Crawford and Knobloch [24]. In fact, the mode which occurs (first primary bifurcation) is either S_o- or S_x-symmetric. The corresponding two neutral curves are plotted in Fig. 3. The aim of this study is to understand how the vertical vibrations will affect these neutral curves. For different values of PrG_v, the graphs of the two first primary bifurcation points are shown in Fig. 4. The values of A_{L_i} are given in Table 3.

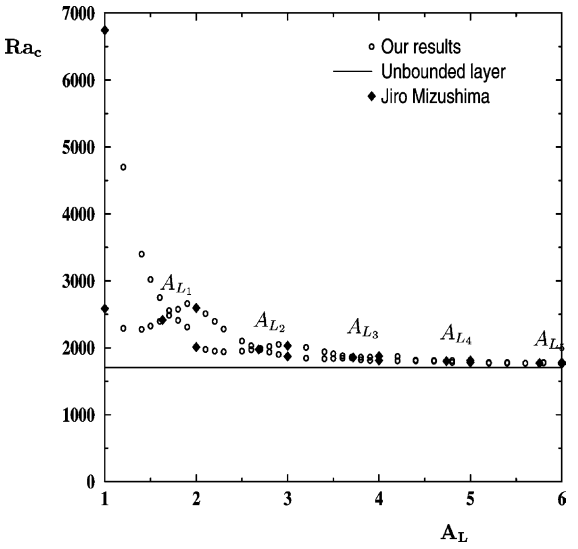

Fig. 3. Critical Rayleigh number Ra_c of the neutral modes S_o and S_x vs. the aspect ratio A_L. Comparison with the results of Mizushima and also with an unbounded layer in the static case. For $A_L < A_{L_1}$ S_o-symmetric one-cell flow, for $A_{L_i} < A_L < A_{L_{i+1}}$ $(i+1)$-cell flow which is S_o- symmetric for i odd or S_x-symmetric for i even.

We note, in Fig. 4, the influence of vertical vibrations on the critical Grashof number. Indeed, the value of critical Grashof number increases with the intensity of vibrations. The conductive solution stays steady for greater temperature differences. The vibrations act both on the stability threshold and on the nature of the flow. We note effectively that the difference $|A_{L_{i+1}} - A_{L_i}|$ rises with the intensity of vibrations. This distance corresponds to the wavelength of the flow in an infinite layer. The stability thresholds translated up and dilated horizontally. Consequently, when the vibrations are not present and considering an aspect ratio of 5, we

Table 1
Convergence with increasing N and M

$N \times M$	2×2	3×2	3×3	4×4	5×5	6×6
Ra_{c_1}	2804.1	2798.0	2645.7	2586.9	2586.1	2585.0
Ra_{c_2}	7806.0	7806.0	7672.4	6752.0	6750.4	6742.5

Critical Rayleigh number Ra_c of the neutral modes S_o (Ra_{c_1}) and S_x (Ra_{c_2}) vs. the couple $N \times M$ for $Pr = 1$, $G_v = 0$ and $A_L = 1$.

Table 2
Convergence with increasing N and M

$N \times M$	2×2	3×2	3×3	4×4	5×5	6×6	8×6	10×6	11×6
Ra_{c_1}	4532.2	2729.1	2733.5	2663.3	2126.3	1861.8	1804.2	1780.3	1778.2
Ra_{c_2}	14602.5	7556.6	4527.3	4144.7	2208.0	2122.0	2021.3	1920.7	1917.8

Critical Rayleigh number Ra_c of the neutral modes S_o (Ra_{c_1}) and S_x (Ra_{c_2}) vs. the couple $N \times M$ for $Pr = 1$, $G_v = 0$ and $A_L = 5$.

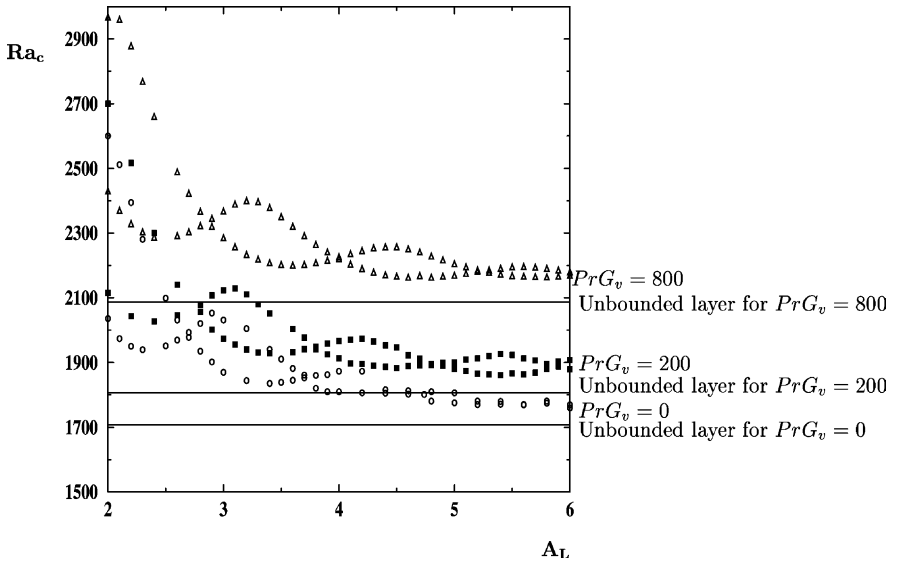

Fig. 4. Critical Rayleigh number Ra_c of the neutral modes S_o and S_x vs. the aspect ratio A_L. We also add the results concerning an unbounded layer. The vertical vibrations increase the value of the critical Rayleigh number.

Table 3
Critical aspect ratios $A_L i$ where the two modes S_o- and S_x-symmetric exchange for $PrG_v = 0$, $PrG_v = 200$ and $PrG_v = 800$

PrG_v	0	200	800
A_{L_1}	1.64	1.65	1.70
A_{L_2}	2.68	2.76	2.86
A_{L_3}	3.72	3.80	4.01

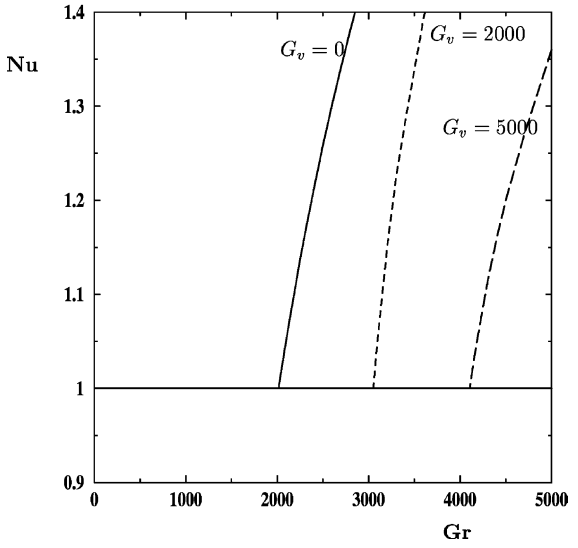

Fig. 5. Bifurcation diagram in the *Nu–Gr* plane for $Pr = 1$, $A_L = 2$ and vertical vibration. Along the two branches plotted for $G_v = 0$ and 2000, the flow is bicellular, whereas for $G_v = 5000$ the flow pattern is monocellular.

note a convective flow with five rolls. For $G_v = 200$, A_{L_4} stays below five and the onset of convective flow still begins with five rolls. Unlike when the intensity of vibration is increasing ($G_v = 800$), the horizontal trans-

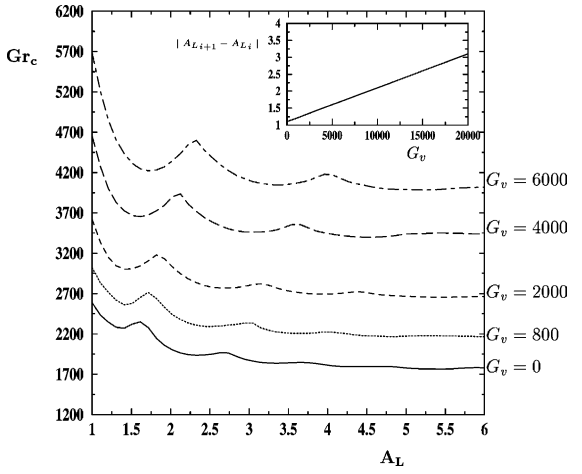

Fig. 6. Stability curves of critical Grashof number Gr_c vs. the aspect ratio A_L for $G_v = 0$, 800, 2000, 4000, 6000. Each bifurcation point is determined on the base of the numerical results obtained for the finite amplitude regimes. We note the influence of vertical vibrations as predicted by theoretical results. Inset: Influence of vibrations on distances $|A_{L_{i+1}} - A_{L_i}|$. Numbers A_{L_i} are relative to the intersection points of the symmetry modes S_o et S_x. These distances increase with the intensity of vibrations and are related to the vibrational Grashof number by the linear evolution law: $|A_{L_{i+1}} - A_{L_i}| = 0.0001\ G_v + 1.1$.

lation on the right of A_{L_4} due to vibrations is sufficient for A_{L_4} to be greater than five. So, we can conclude that the setting off of the convective motion is characterized by a four-roll regime. These results are confirmed by the numerical results (Figs. 5 and 6). Each point in Fig. 6 was obtained by plotting the complete bifurcation diagram as in Fig. 5 and noting the value of Ra_c.

4. Computations of finite amplitude regimes

4.1. Numerical method

The system of Eqs. (12)–(16) was solved numerically using a spectral method. This is based on the projection–diffusion algorithm developed for solving the 2*D*–3*D* unsteady incompressible equations [25]. Its interest is to circumvent the difficulty posed by the gradient pressure at the borders of the cavity. Temporal integration consists of a semi-implicit second-order finite difference approximation. The linear (viscous) terms are treated implicitly using a second-order backward Euler scheme, while a second-order Adams–Bashforth scheme is employed for the nonlinear (advective) parts. When applied to an advection–diffusion equation such as

$$\frac{\partial f}{\delta t} + \mathbf{U}\cdot\nabla f = \alpha\Delta f \tag{57}$$

the method leads to

$$\frac{\frac{3}{2}f^{n+1} - 2f^{n} + \frac{1}{2}f^{n-1}}{\delta t} = \alpha\Delta f^{n+1} - 2(\mathbf{U}\cdot\nabla f)^{n} - (\mathbf{U}\cdot\nabla f)^{n-1} \tag{58}$$

This equation can be written in the following form of the Helmholtz equation

$$(\Delta - h)f^{n+1} = s \tag{59}$$

where $h = \frac{3}{2\alpha\delta t}$ is the Helmholtz constant and s is a scalar quantity containing all the terms known at time $t_n = n\delta t$ (n is the time level and δt is the time step). The temporal integration, therefore, transforms the systems into a Helmholtz problem arising from Eq. (14) coupled to the Poisson problems (15), (16) with appropriate boundary conditions. Eqs. (12) and (13) are transformed into a generalized Stokes problem and solved by the projection–diffusion method of Khallouf [26]. All the subproblems obtained are either Helmholtz or Poisson-like operators. A spectral method, namely one utilizing Legendre collocation points, is used in the spatial discretization of the Helmholtz and Poisson-like operators. Successive diagonalization is implemented to invert these operators. We mention that the Stokes and Darcy–Euler solvers are direct and guarantee an accurate spectral solution with divergence-free solenoidal fields over the entire domain, including the boundaries.

4.2. Vertical vibration

Fig. 5 represents the Nusselt vs. the Grashof number for $Pr = 1$ and $A_L = 2$. As G_v increases, the stability threshold increases too. Hence, vertical vibrations have a stabilizing effect on convective flow. As the first primary bifurcations are supercritical pitchforks with either S_o-symmetric or S_x-symmetric solutions, a weakly nonlinear analysis arround the bifurcation point shows that

$$Nu = K\sqrt{(Gr - Gr_c)}$$

where K is a constant which depends on G_v [14]. For each value of G_v, as $Nu^2 = K(Gr - Gr_c)$, a simply extrapolation technique allows us to determine an accurate value of Gr_c. We use the finite amplitude results to plot the Fig. 6.

Fig. 6 computed for $G_v = 0$, 800, 2000, 4000 and 6000 represents the analogue of Fig. 4 which summarizes the theoretical results. The numerical results confirm all the theoretical ones. With the vibrations, the curves are translated up and dilated horizontally. This means that the vertical vibrations delay the onset of the convection and have a stabilizing effect on the convective flow. We can better understand the dilating effect due to vibrations by looking at the inset in Fig. 6. This shows that the critical distance $|A_{L_{i+1}} - A_{L_i}|$ is a linear function of the vibrational Grashof number and, consequently, the distance increases with the intensity of vibrations.

4.3. Imperfect bifurcation

We deal now with an inclination of the axis of vibration from the vertical (Fig. 7). Computations were performed for a rectangular cavity ($A_L = 2$) for ($G_v = 0$, 2000, 5000, 10,000 and 20,000). Our previous prediction, given by the linear theory in which there is no conductive solution when the axis of vibration diverges from the temperature gradient, is confirmed here. Indeed, for $\alpha = \frac{\pi}{2} - \frac{1}{100}$ and when the intensity of vibrations increases ($G_v = 2000$), we can observe quasi-conductive motion or weak convection in the cavity. The deviation of the stability curve drawn for ($G_v = 2000$, 5000, 10,000, 20,000) from the stability curve ($G_v = 0$) proves that there is no equilibrium solution for $\alpha \neq \frac{\pi}{2}$. This is an imperfect bifurcation scenario. When the vibrational Grashof number increases markedly and attains a critical vibrational Grashof number, the critical Grashof number begins to diminish in comparison with the previous results. This shows that, at a certain value of intensity of vibration, the vibrations have a destabilizing effect on the convection.

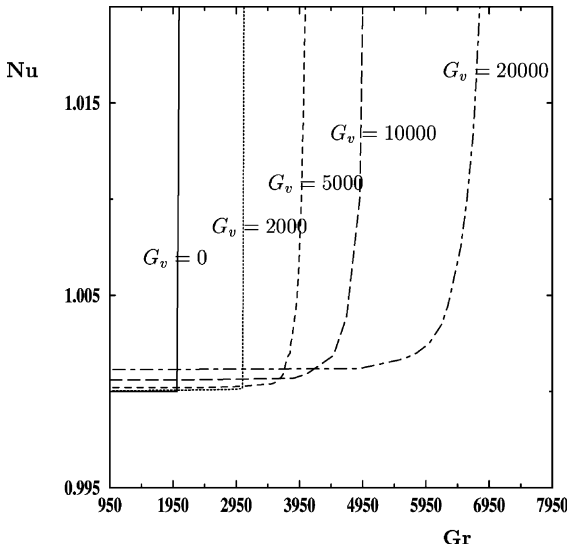

Fig. 7. Influence of a small deviation from the special case of vertical vibration. Bifurcation diagram in the *Nu–Gr* plane for $Pr = 1$, $A_L = 2$ and $\alpha = \frac{\pi}{2} - \frac{\pi}{100}$.

4.4. Horizontal vibration

The results for horizontal vibrations ($\alpha = 0$) have been summarized in (Fig. 8) for $Pr = 1$ and $A_L = 2$. This kind of vibration is very effective in driving thermovibrational convection. This is the case of non-equilibrium. When G_v increases for example for ($G_v = 2000$), a small temperature difference applied to the horizontal walls can set off a weak convection movement. The quasi-conductive regime generated is, therefore, destabilized for a critical Grashof number below the stability threshold of the conductive regime ($G_v = 0$). The critical Grashof number continues to decrease with increasing vibrational Grashof number (inset Fig. 8). In microgravity, a convective regime is present in the cavity and increases with the intensity of vibrations.

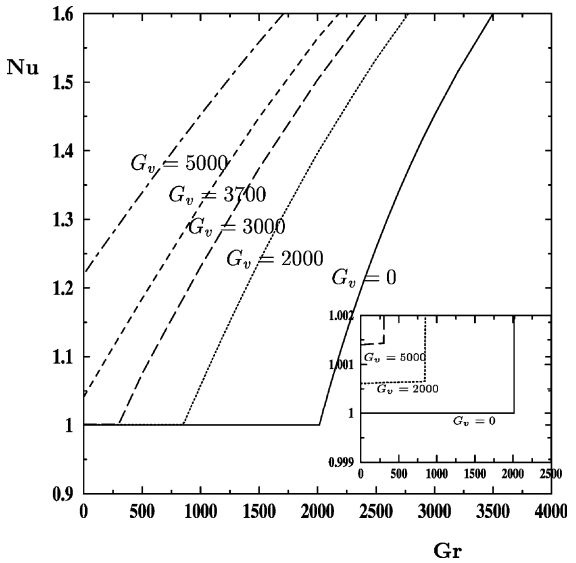

Fig. 8. Bifurcation diagram in the *Nu–Gr* plane for $Pr = 1$, $A_L = 2$ and horizontal vibration. Along all the branches plotted for $G_v = 0$, 2000, 3000, 3700, 5000 the flow is bicellular. The next figure displays an enlargement around the quasi-diffusive regime ($Nu = 1$). Inset: enlargement around the quasi-diffusive regime ($Nu = 1$) for horizontal vibration. Along all the branches plotted for $G_v = 0$, 2000, 3000, the flow is bicellular.

5. Conclusion

The influence of vibrations of low amplitude and high-frequency on fluid subjected to a temperature difference has been studied. In order to better understand these effects of vibration in both intensity and direction, we have described a theoretical and numerical study of thermovibrational convection in an infinite layer, in a square, and in a rectangular cavity, notably in the particular case permitting the existence of an equilibrium or quasi-equilibrium state. We noted close agreement between the theoretical and the numerical results. In presence of vibrations, an infinite layer cannot perfectly represent the physical phenomena observed in very long rectangular cavities. In fact, the wall contribution is significant because it implies that mechanical equilibrium is impossible when the axis of vibrations is not along the temperature gradient. When $\alpha \neq \frac{\pi}{2}$, the vibrations generate a convective flow for temperature differences below those necessary for the generation of convection in the classical Rayleigh–Benard problem. As these vibrations are sufficiently intense, it is possible to set off convection in a microgravity environment (space stations). This environment is dynamic and reveals three-dimensionnal accelerations known as g-jitters having frequencies varying between 10^{-1} and 10^{3} Hz, which can perturb the realization of experiments like the measurement of the Soret coefficient or the making of pure cristals. On the other hand, when the axis of vibration is vertical, vibrations can preserve the conductive regime above the classical threshold of Rayleigh–Benard. We can conclude that it is possible to generate or suppress the convective regime created by thermal gradient by means of mechanical vibrations. Thermal control with the use of vibrations is then possible.

Acknowledgement

We thank G. Couegnas for his work and his contribution to the present study.

References

[1] I.B. Simonenko, S.M. Zen'kovskaja, On the effect of high-frequency vibrations on the origin of convection, Izv. Akad. Nauk SSSR. Ser. Meh. Zhidk. Gaza 5 (1966) 51–55.

[2] I.B. Simonenko, A justification of the averaging method for a problem of convection in a field rapidly oscillating forces and other parabolic equations, Mat. Sb. (129) 2 (1972) 245–263.

[3] G.Z. Gershuni, E.M. Zhukhovitskii, Free thermal convection in a vibrational field under conditions of weightlessness, Sov. Phys. Dokl. 24 (11) (1979) 894–896.

[4] L.M. Braverman, A. Oron, On the oscillatory instability of a fluid layer in a high-frequency vibrational field in weightlessness, Eur. J. Mech. 13 (1) (1994) 115–128.

[5] G.Z. Gershuni, E.M. Zhukhovitskii, vibration-induced thermal convection in weightlessness, Fluid Mech. Sov. Res. 15 (1) (1986) 63–84.

[6] M.P. Zavarykin, S.V. Zorin, G.F. Putin, Convective instabilities in a vibrational field, Dokl. Akad. Nauk SSR 299 (1998) 174–176.

[7] D.D. Richardson, Effect of sound and vibration on heat transfer, Appl. J. Mech. Rev. 20 (1967) 201–217.

[8] R.E. Forbes, C.T. Carley, C.J. Bell, Vibration effects on convective heat transfer in enclosures, J. Heat Transfer 92 (1970) 429–438.

[9] Y.S. Yurkov, Vibration induced thermal convection in a square cavity in weightlessness (finite frequencies), Convective Perm Teachers (1981) 98–103.

[10] W.S. Fu, W.J. Shieh, A study of thermal convection in an enclosure induced simultaneously by gravity and vibration, Int. J. Heat Mass Transfer 35 (7) (1992) 1695–1710.

[11] G.Z. Gershuni, E.M. Zhukhovitskii, Y.S. Yurkov, Vibrational thermal convection in rectangular cavity, Trans. Acad. Sci. SSSR (Izvetiya), 4, Mech. Zhidk. Gaza, 1982.

[12] H. Khallouf, G.Z. Gershuni, A. Mojtabi, Numerical study of two-dimensional thermovibrational convection in rectangular cavities, Num. Heat Transfer 27 (Part A) (1995) 297–305.

[13] A. Lizée, Contribution à la convection vibrationnelle, contrôle actif de la convection naturelle, Thèse de doctorat de l'Université d'Aix-Marseille II, 1995.

[14] G. Bardan, E. Knobloch, A. Mojtabi, H. Khallouf, Natural doubly diffusive convection with vibration, Fluid Dynam. Res. 28 (2001) 159–187.

[15] P.M. Gresho, R.L. Sani, The effects of gravity modulation on the stability of a heated fluid layer, J. Fluid Mech. 40 (1970) 783–806.

[16] S. Rosenblat, G. Tanaka, Modulation of thermal convection instability, Phys. Fluids 14 (1971) 1319–1322.

[17] S. Biringen, G. Danabasoglu, Computation of convective flow with gravity modulation in rectangular cavities, J. Thermophys. 4 (1990) 357–365.

[18] R. Monti, R. Savino, Microgravity experiments acceleration tolerability on space orbiting laboratories, J. Spacecraft Rockets 33 (1996) 707–716.

[19] R. Monti, R. Savino, Influence of g-jitter on fluid physics experimentation on board the International Space Station, in: Symposium Proceedings on Space Station Utilisation, Darmstadt, Germany, 1996, pp. 215–224.

[20] R. Savino, R. Monti, M. Piccirillo, Thermovibrational convection in a fluid cell, Comput. Fluids 27 (1998) 923–939.

[21] G.Z. Gershuni, D.V. Lyubimov, Thermal Vibrational Convection, Wiley, 1998.

[22] W.H. Reid, D.L. Harris, Some further results on the Bénard problem, Phys. Fluids 1 (1958) 102–110.

[23] J. Mizushima, Onset of thermal convection in a finite two-dimensional box, J. Phys. Soc. Jpn. 64 (1995) 2420–2432.

[24] J.D. Crawford, E. Knobloch, Symmetry and symmetry-breaking bifurcation in fluid dynamics, Annu. Rev. Fluid Mech. 23 (1991) 341–387.

[25] S.A. Orszag, M. Israeli, M.O. Deville, Boundary conditions for incompressible flows, J. Scientific Comput. 1 (1986) 75–111.

[26] H. Khallouf, Simulation numérique de la convection thermo-vibrationnelle par une méthode spectrale, Thése de doctorat de l' Université Paul Sabatier, Toulouse III, 1995.